J. Synchrotron Rad. (1998). **5**, 1258–1262

Anomalous Wide-Angle X-ray Scattering Apparatus on the GILDA Beamline at the ESRF

C. Meneghini,[a,b]* A. Balerna,[a] F. Boscherini,[a] S. Pascarelli[b] and S. Mobilio[a,c]

[a]Istituto Nazionale di Fisica Nucleare (INFN), PO Box 13, I-00044 Frascati, Italy, [b]Istituto Nazionale di Fisica della Materia (INFM), Corso Perrone 24, I-16152 Genova, Italy, and [c]Dipartimento di Fisica, 'E. Amaldi' Università di Roma Tre, Via della Vasca Navale 84, I-00146 Roma, Italy. E-mail: cmeneghi@1nf.infn.it

(*Received 20 November 1997; accepted 6 May 1998*)

The experimental apparatus for anomalous wide-angle X-ray scattering (AWAXS) on the GILDA beamline at the ESRF is described. The main features are the high beam stability and reproducibility which allow anomalous scattering effects to be resolved also on dilute elements, the large spectral range which allows AWAXS experiments at the *K* edges of heavy elements, and the use of a high-efficiency detection system. The apparatus has been tested in extreme conditions by performing AWAXS experiments at the Eu *K* edge in Eu-doped Sr metaphosphate glasses.

Keywords: anomalous wide-angle X-ray scattering (AWAXS); high energy.

1. Introduction

The anomalous wide-angle X-ray scattering (AWAXS) technique (Fuoss *et al.*, 1981; Materlik *et al.*, 1994, and references therein) is a powerful tool in the study of amorphous multi-component systems like alloys or doped samples. It uses the sharp variation of the atomic scattering factors near the absorption edge of a particular atomic species to obtain detailed information on the local structure around that species. Synchrotron radiation is the ideal source for AWAXS experiments: its wide spectral range allows the study of many elements; working at high energy, spectra up to large values of the exchanged momentum (q) can be measured, thus achieving a high resolution in the radial distribution functions; moreover, high beam stability and reproducibility, as well as the intense photon flux on samples, allow weakly scattering systems like dilute samples to be studied.

In the present paper we describe the apparatus for AWAXS installed on the GILDA (general purpose Italian beamline for diffraction and absorption) (Pascarelli *et al.*, 1995, 1996) beamline at the European Synchrotron Radiation Facility (ESRF) which allows studies on amorphous and liquid systems in the wide energy range between 8 keV and over 50 keV.

2. Beamline description

GILDA collects 4 mrad of radiation emitted by a bending magnet of the ESRF (critical energy 19.2 keV). The beamline consists of four sections: an optics hutch and three experimental hutches in series. In the optics hutch the beam is monochromated in a wide energy range (5–50 keV) and focused in the horizontal and vertical plane, providing an intense photon beam of average flux 10^{11} photons s^{-1} and an energy resolution in the range 10^{-4}–10^{-5}. X-ray absorption and scattering experiments are performed in the three experimental hutches.

In the optics hutch a cooled slits system (horizontal and vertical) at 27 m from the source defines the incident beam size. A high-pass filter system, composed of C, Al and Cu interchangeable foils of different thickness, cuts off the low-energy tail of the synchrotron emission reducing the thermal load on the subsequent optical elements. The optics works in two different configurations: the high-energy configuration and the high-flux/high-resolution configuration.

In the high-energy configuration only a double-crystal fixed-exit monochromator is used; mounting Si[311] crystals, a monochromated beam in the energy range 5–32 keV is achieved; with an Si[511] crystal set the spectral range extends up to 50 keV. The horizontal focusing of the beam is achieved by bending the monochromator second crystal in the sagittal plane (Pascarelli *et al.*, 1995). The focal spot dimensions are kept fixed during an energy scan by continuously adjusting the crystal curvature (dynamical focusing). The angular alignment of the two crystals is finely adjusted with a piezoelectric crystal driven by a PID feedback circuit, monitoring the photon flux just in front of the sample; this system produces an excellent positional stability of the beam.

The high-flux/high-resolution geometry covers the energy range 5–28 keV; two grazing-incidence mirrors are used to focus the beam in the vertical plane and to increase the resolution and transmission of the monochromator. Two coatings are available on both mirrors: Pd and Pt. The

first mirror, upstream of the monochromator and with a fixed radius of curvature (16 km), collimates the beam vertically, thus increasing the transmission and resolution of the monochromator. The second mirror, downstream of the monochromator, has an adjustable focal length between 5 and 15 km to vertically focus the beam in the three experimental hutches. Besides focusing, the mirrors also provide low-pass filtering of the beam (cut-off at about 24 keV and 28 keV for Pd and Pt, respectively).

In the first experimental hutch, X-ray absorption (XAFS) experiments in transmission, fluorescence and total reflection (refle-XAFS) are performed; this hutch is in a 1:3 geometry with respect to the monochromator to obtain the maximum flux. In the second hutch, the two-circle diffractometer for AWAXS is installed; the apparatus is in approximately 1:1 geometry to reduce optical aberrations. In the third hutch, non-permanent apparatus can be installed for non-standard experiments.

In the diffraction hutch a photon flux of 10^{10}–10^{11} photons s^{-1} in the energy range 8–50 keV is achieved; thanks to the sagittal focusing, the horizontal spot width is less than 3 mm. As for the vertical dimensions, in the high-flux/high-resolution optical configuration the vertical spot size is $\leq$2 mm. This size can be reduced using vertical slits. Without mirrors the vertical size is defined by the slits system only.

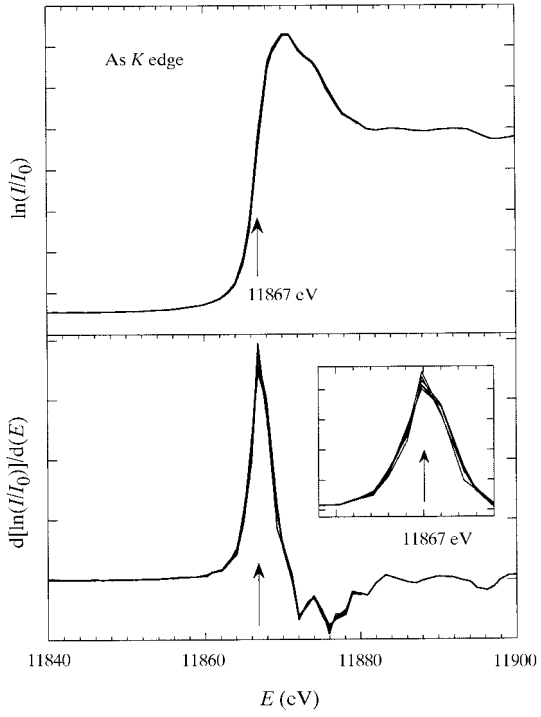

Figure 1
Tests of the stability and reproducibility of the GILDA optics. The top panel reports the near-edge absorption spectra of a GaAs sample recorded every 20 min; the good data reproducibility is better evidenced in the lower panel plots reporting their derivatives. The edge position is reproduced within $\pm$0.5 eV at 11.867 keV giving an energy reproducibility better than 10^{-4}.

The energy stability of the incident beam is crucial for AWAXS, especially during near-edge data acquisition when even a small energy drift introduces distortions into the spectra, providing unreliable results. Fig. 1 reports six absorption edges [$\ln(I/I_0)$] of a GaAs reference sample with their derivative, measured at intervals of 20 min. The edge position is reproduced within $\pm$0.5 eV. Stability of the same order has been observed over longer periods (>10 h). No drift due to storage-ring refilling has been observed. This ensures an excellent stability during the measurement time of a single energy diffraction scan (typically 4–12 h).

3. The AWAXS apparatus

Fig. 2 reports the experimental set-up for AWAXS experiments on amorphous systems. It consists of a two-circle (ω–2θ) horizontal-axis goniometer (G), a sample holder (H) on the ω goniometer circle, a solid-state multidetector (MD) to record diffracted intensity, a detector (I_0) to monitor the incident beam intensity for data normalization, and the slit systems (S1 and S2) to define the beam size on the sample. The two-circle goniometer, Seifert model MZ IV, has an angular resolution of 0.28" (1.4 μrad) and an absolute reproducibility of 2" (9.7 μrad); it is mounted on a kinematical base (KB) to align the goniometer on the beam. Samples are aligned on the goniometer using a motorized head. A large choice of sample holders allows the matching with many experimental requirements: to use both reflection and transmission scattering geometries, to measure liquid samples, to reduce air scattering using a vacuum chamber, and to install an oven for high-temperature studies (up to 1773 K). The resolution slits (four tungsten blades) (S1) define the beam

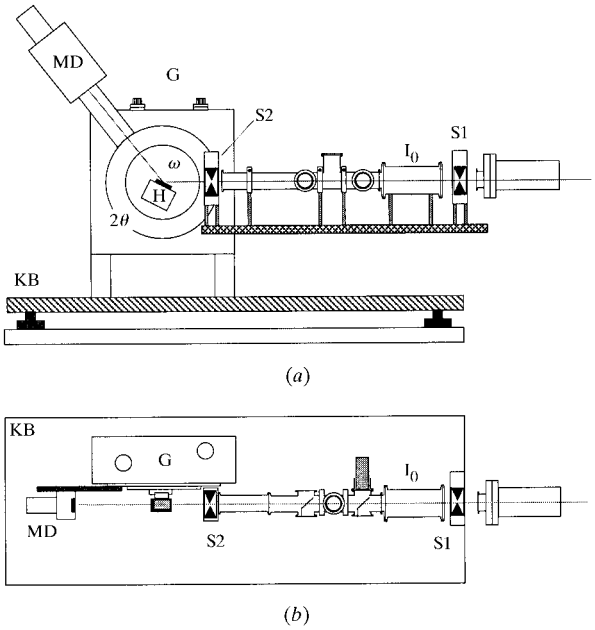

Figure 2
The GILDA diffractometer. (*a*) Side view. (*b*) Top view.

size on the sample with an accuracy of ±25 μm. The four-blade slit system (S2) (antiscattering slits) placed near the sample removes spurious scattering effects. All the apparatus can be moved in the vertical direction, to follow the beam, whose height changes by about 45 mm between the two optical configurations of the beamline (with and without mirrors), and in the horizontal direction to remove all the apparatus from the beam.

The diffracted beam is recorded by a 16-element solid-state multi-detector (MD), provided by DAM (Développement Analyses et Mesures, Paris), mounted on the 2θ goniometer arm at 50 cm from the sample. It is composed of 16 Si(Li) solid-state elements (Fig. 3) covering an angular range of about 15° with an angular resolution of 0.22°; the rather high thickness of the active layer of the Si(Li) elements (6 mm) ensures a detection efficiency higher that 90% up to 25 keV and of 30% at 50 keV. The detector energy resolution is enough to separate the elastic and $K\alpha$ and $K\beta$ fluorescence lines at photon energies far above an absorption edge. When using photon energies close to the absorption edge, the energy resolution does not allow either the Kβ fluorescence or Compton scattering to be resolved. The removal of these inelastic contributions from the data is made by estimating the intensity of the $K\beta$ fluorescence from that of the $K\alpha$ fluorescence, according to Laridjani *et al.* (1987), and by evaluating the Compton scattering contribution from theoretical tables (Palinkas, 1973; Hajdu, 1971).

3.1. *A multi-window analyzer for multi-element detectors*

Fig. 4 reports the 'parallel'-processing readout scheme of the 16 signals coming from the Si(Li) elements. The charge signal from each detector, amplified to a Gaussian shape through a charge preamplifier and a spectroscopy amplifier (Silena 542), is processed by a multi-window analyzer described below; its TTL output pulses are stored in a counter and then recorded in a data file. The 'test signal' input of the preamplifier stage is used to estimate count-loss effects due to pile up and dead time.

The biggest problem in using solid-state detectors is the non-linearity in the response at high counting rates; this reduces the dynamic range in which these detectors are usable. The magnitude of the anomalous scattering effect is about 10^{-2} of the elastic signal so the non-linearity and statistical noise on data must be kept at least one order of magnitude better, *i.e.* 10^{-3}. Two main effects give rise to non-linearity: pulse pile-up in the amplifier and dead time in the pulse-height analysis (Knoll, 1989). These two effects limit the usable counting rate typically to a few 10^3 counts s^{-1}. This is a serious problem since it does not allow the use of the high flux available on the beamlines of third-generation synchrotron radiation machines; moreover, with such counting rates, long acquisition times are required to reduce the Poisson noise. To avoid the dead time due to the pulse-height analysis we developed a multi-

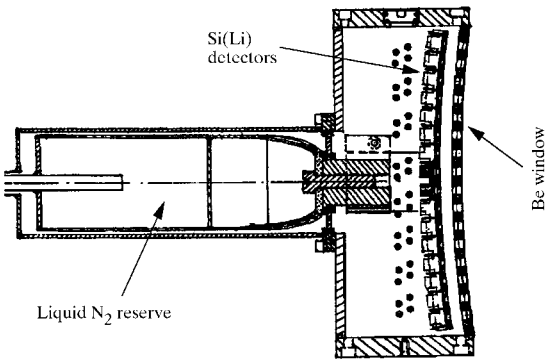

Figure 3
The 16-element Si(Li) multidetector.

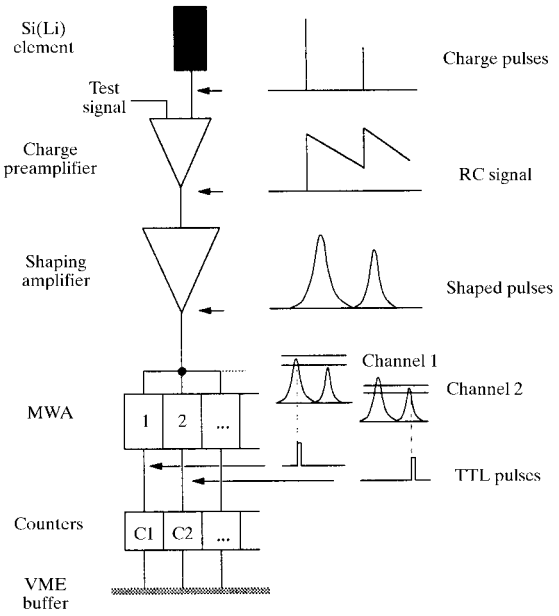

Figure 4
Schematic view of the multiwindow analyzer.

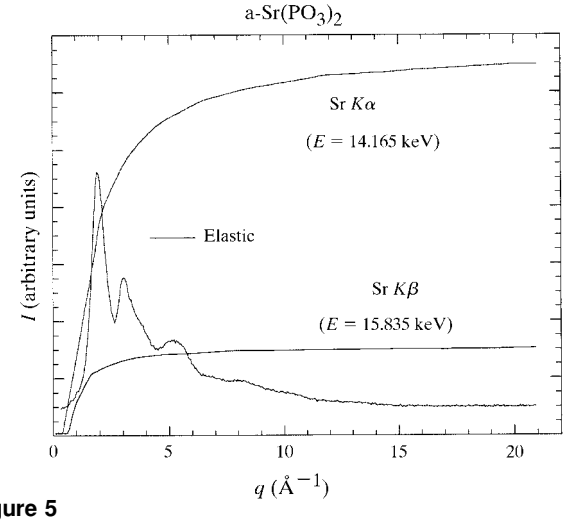

Figure 5
An example of data acquisition on one Si(Li) detector: elastic and fluorescence contributions are recorded at the same time, as described in text.

window analyzer (MWA). It consists of a set of 16 independent single-channel programmable window analyzers (SCA) that process in parallel the shaped pulses from the amplifiers. In such a way, 16 different signal levels can be monitored at the same time. Any combination is possible as 16 different windows monitoring signals from the same detector or one window for each detector or other combinations. The dead time of the MWA was measured with a random pulse generator simulating the input signals at the preamplifier stage and using 1 μs of amplifier shaping time. MWA windows were at 20% of the pulse height. The output frequency as a function of the input rate was fitted to a 'paralyzable' detector model curve (Knoll, 1989) giving a dead time of 4 ± 0.5 μs. The obtained values show that the time required by the MWA for signal processing and data storage is negligible (~1 μs) so only the dead time due to the shaping amplifier contributes. Therefore, our MWA readout system is a factor of two or three faster than a standard system. During AWAXS measurements, four SCAs are combined to read at the same time the elastic and fluorescence ($K\alpha$, $K\beta$) (Fig. 5) and the total counting rate on each detector. The fourth SCA also reads the test signal to check for non-linearity.

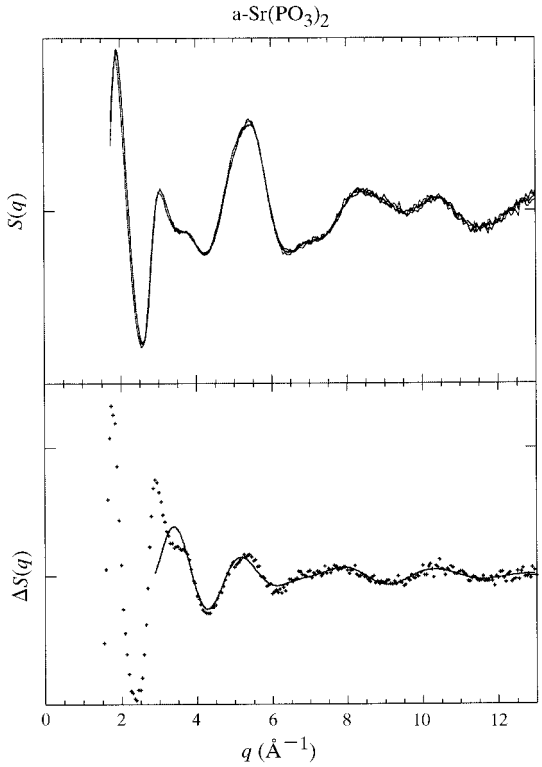

Figure 6
The top panel reports three total structure factors for an a-$Sr(PO_3)_2$ sample recorded on different Si(Li) elements and in successive runs in order to check the reproducibility of the experimental set-up and of the data treatment procedures. The lower panel reports the Sr differential structure factor in the a-$Sr(PO_3)_2$ sample obtained using $S(q)$ near (16.097 keV) and below (15.800 keV) the Sr K edge. In total, 48 $S(q)$ have been recorded for each energy (12–16 h of beam time/energy). The full line is the first-shell contribution to $\Delta S(q)$ obtained by fitting the first peak of $\Delta g(r)$.

3.2. *Experimental check of the AWAXS apparatus*

To illustrate the performances of the whole apparatus, we show here AWAXS data obtained on pure and Eu-doped Sr metaphosphate glasses at the Sr and Eu K edges (Bionducci *et al.*, 1996). The upper panel in Fig. 6 reports three total structure factors (TSF) measured at 15.800 keV (207 eV below the Sr K edge) on an amorphous $Sr(PO_3)_2$ sample in different runs and from different Si(Li) detectors. A very good agreement between the data set with a standard deviation between the different $S(q)$ lower than 5×10^{-3} was achieved. The high quality of the data allowed us to obtain a high-quality differential structure factor $\Delta S(q)$ as shown in the lower panel of Fig. 6.

A feature of the GILDA beamline is its ability to work up to 50 keV. At such high energies a wide reciprocal space is achieved resulting in a better R-space resolution. Moreover, AWAXS at such energies is of great interest since many elements have K edges in the region between 30 and 50 keV. For these elements, measurements at L edges (*i.e.* at $E \leq 10$ keV) give a poor R-space resolution. Fig. 7 reports data obtained at the Eu K edge on Eu-doped a-$Eu_{0.1}Sr_{0.9}(PO_3)_{2.1}$ (Bionducci *et al.*, 1996). This experiment was an original attempt to perform AWAXS at such high energies, with additional difficulties for the low atomic concentration of Eu (1.2%). TSFs were obtained at different beam energies (25, 46, 48.48 and 54 keV) using both Si[511] flat and Si[933] sagittally bent crystals. The comparison of high-energy data with those obtained at 25 keV is excellent: all the TSFs are almost identical (the small anomalous effect cannot be seen at this level).

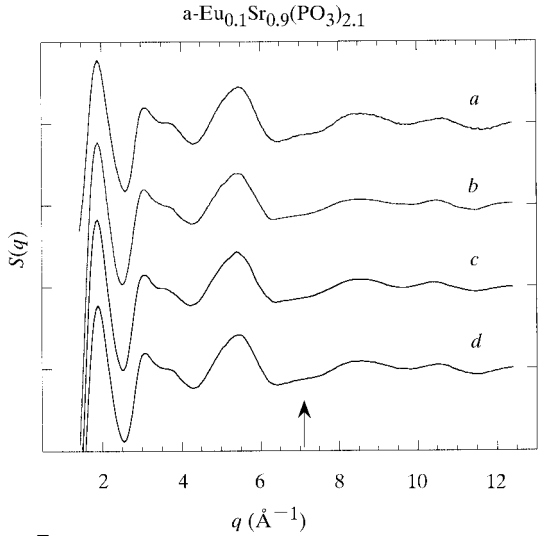

Figure 7
High-energy measurements: $S(q)$ obtained at (*a*) 25 keV, (*b*) 46 keV, (*c*) 48.480 keV and (*d*) 54 keV. Si[311] monochromator crystals have been used for (*a*), the third-harmonic reflection Si[933] has been used for (*c*) and (*d*), and Si[511] crystals were employed for (*b*). The arrow indicates the maximum momentum transferred reachable using Eu L-edge energy.

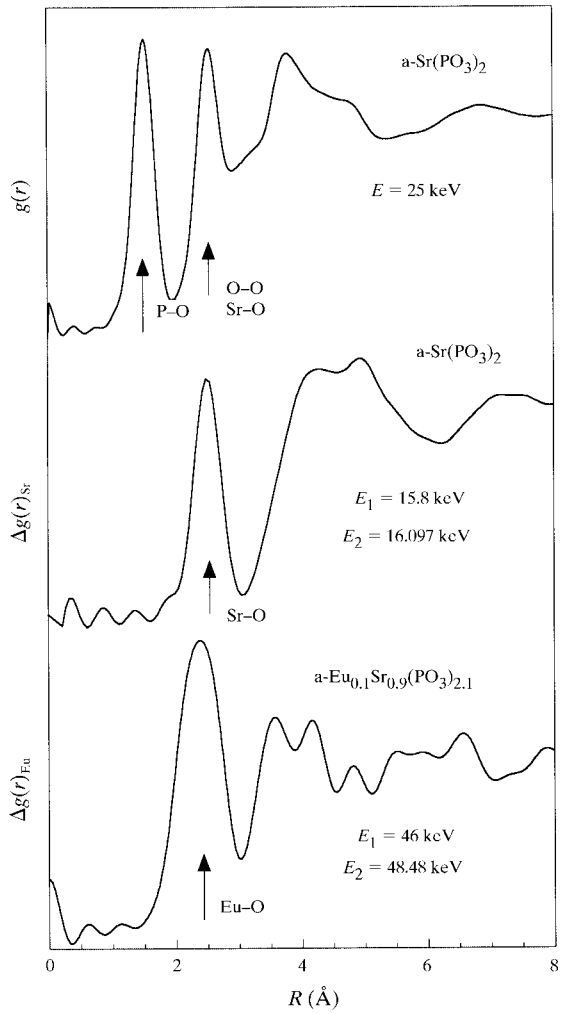

Figure 8
AWAXS results: the pair-correlation function $g(r)$ of the undoped a-$Sr(PO_3)_2$ (upper plot) is compared with the differential pair-correlation functions $\Delta g(r)_{Sr}$ (middle plot) measured at the Sr K edge. $\Delta g(r)_{Eu}$ (lower plot) is obtained on the doped sample at the Eu K edge. The first peak of $g(r)$, at about 1.6 Å, represents the P—O shell of the phosphate matrix, while the second peak represents the O—O and Sr—O shell contributions. The first peaks of $\Delta g(r)_{Sr}$ and $\Delta g(r)_{Eu}$ represent the Sr—O and Eu—O coordination shells, respectively.

In Fig. 8 we compare the total pair-correlation function, $g(r)$, of the undoped Sr metaphosphate sample measured at 25 keV with the differential pair-correlation function $\Delta g(r)_{Sr}$ obtained at the Sr K edge on the same sample, and with $\Delta g(r)_{Eu}$ obtained from data at the Eu K edge in the Eu-doped sample. The main results obtained from a quantitative analysis are (Balerna *et al.*, 1998; Bionducci *et al.*, 1996; Meneghini, 1996): the metaphosphate host matrix is unchanged upon doping; the average coordination number for Sr of ~5 suggests an irregular distribution of the first coordination shell or an equal number of fourfold- and sixfold-coordinated Sr; and the coordination number for the Eu—O shell, ~8.5, is in good agreement with EXAFS results. This cross check demonstrates that good quality AWAXS data can be obtained at high energies and on weakly concentrated elements.

4. Conclusions

We have described the anomalous scattering apparatus of the GILDA beamline. The main features are the large spectral range which allows AWAXS to be performed at the K edges of heavy elements, the high beam stability and reproducibility which allow anomalous scattering effects to be resolved also for diluted elements, and an efficient detection system. Measurements performed on a-$Eu_{0.1}Sr_{0.9}(PO_3)_{2.1}$ at high energy (Eu K edge) and at a low atomic concentration were a strong check of the experimental set-up.

We are grateful to G. Navarra and M. Bionducci for stimulating discussions and to Professor G. Licheri for encouraging suggestions. We acknowledge the excellent technical support of F. Campolungo, L. Sangiorgio, V. Sciarra and V. Tullio (INFN-LNF). The experimental help of F. D'Acapito and S. Colonna in running the beamline is greatly appreciated. GILDA beamline is financed by the Italian institutions CNR, INFM and INFN.

References

Balerna, A., Bionducci, M., Falqui, A., Licheri, G., Meneghini, C., Navarra, G. & Bettinelli, M. (1998). *J. Non-Cryst. Solids.* In the press.
Bionducci, M., Meneghini, C., Navarra, G., Licheri, G., Balerna, A. & Mobilio, S. (1996). *Proc. MRS Spring 96*, **437**, 161–167.
Fuoss, P. H., Eisenberger, P., Warburton, W. K. & Bienenstock, A. (1981). *Phys. Rev. Lett.* **46**, 1537.
Hajdu, F. (1971). *Acta Cryst.* A**27**, 73–76.
Knoll, G. F. (1989). *Radiation Detection and Measurement.* New York: Wiley.
Laridjani, M., Sadoc, J. F. & Raux, D. (1987). *J. Non-Cryst. Solids*, **91**, 217–234.
Materlik, G., Sparks, C. J. & Fischer, J. (1994). *Resonant Anomalous X-ray Scattering Theory and Applications.* Amsterdam: Elsevier Science.
Meneghini, C. (1996). PhD thesis, University of Rome 'Tor Vergata', Italy.
Palinkas, G. (1973). *Acta Cryst.* A**29**, 10–12.
Pascarelli, S., Boscherini, F., D'Acapito, F., Hrdy, J., Meneghini, C. & Mobilio, S. (1996). *J. Synchrotron Rad.* **3**, 147–155.
Pascarelli, S., D'Acapito, F., Antonioli, G., Balerna, A., Boscherini, F., Cimino, R., Dalba, G., Fornasini, P., Licheri, G., Meneghini, C., Rocca, F. & Mobilio, S. (1995). *ESRF Newsl.* **23**, 17–19.